Dynamic Studies of the Molecular Relaxations and Interactions in Microcomposites Prepared by In-Situ Polymerization of Silicon Alkoxides

John J. Fitzgerald,* Christine J. T. Landry, and John M. Pochan

Eastman Kodak Company, Rochester, New York 14650-2135

Received November 26, 1991; Revised Manuscript Received March 13, 1992

ABSTRACT: In-situ polymerization of silicon alkoxide was used to prepare composites of silicon dioxide and poly(vinyl acetate) (PVAc). The local environment of the PVAc chains was probed using FTIR, dielectric, and dynamic mechanical spectroscopy. Dielectric relaxation master curves were prepared, and the dielectric data were fit to the empirical Kohlrausch–Williams–Watts function (KWW). The results showed that β decreased with increasing sol–gel concentration, indicating that there is a broadening in the distribution of relaxation times for PVAc chains. The results suggest that there exists an interfacial region in the composites where the mobility of the PVAc is reduced by the interactions with the silicate network. In addition, at high concentrations of tetraethoxysilane (TEOS) it was not possible to shift the data because of a breakdown of time–temperature superposition. Further, at these concentrations a plateau region above T_g was observed by dynamic mechanical analysis. The results show that the silicate network inhibits the relaxation of at least a portion of the PVAc chains, and it is believed that the plateau is a manifestation of the PVAc chains that are entrapped in a continuous silicate network and of the nature of the network itself. It was also shown that the distribution of relaxation times narrows as the cure temperature increases. In addition, as the composite is cured, the amount of hydrogen bonding between the PVAc and the silicate network decreases. This is presumably due to further condensation of the silicate and the proportional decrease in the amount of available silanol groups.

Introduction

The incorporation of inorganic oxides into organic polymeric materials via the in-situ polymerization of inorganic alkoxides by the sol–gel process is of growing interest in both industry and academics as evidenced by the number of publications in the area. In particular, a great deal of work has been done recently by Schmidt et al.,[1,2] Coltrain et al.,[3] Wilkes et al.,[4–7] Mark et al.,[8–11] and Mauritz et al.[12,13] In these reports, several methods have been utilized to promote compatibility between the inorganic network and either an inorganic or organic polymer. These methods include reacting an orthosilicate directly with organic polymers or oligomers that are end-capped with or that contain functional groups capable of entering into a cross-reaction with the inorganic polymers.[3–7] Also, the inorganic polymer may be introduced by swelling an organic or inorganic polymer network with the metal alkoxide and precipitating the metal oxide in situ.[1,2,8–11]

There are some polymers, however, which have been found to exhibit inherent affinity for inorganic oxides through some type of specific interaction such as, but not limited to, hydrogen bonding. Optically clear composites can be prepared by taking advantage of these interactions and choosing the proper organic–inorganic system.[14] Organic polymers that contain functional groups such as carbonyls or ether oxygens have been shown to exhibit hydrogen-bonding interactions with the silicon oxide networks formed by the acid-catalyzed polymerization of silicon alkoxides. Such polymers are poly(methyl methacrylate) (PMMA),[14c,15,16] poly(vinyl acetate) (PVAc),[16–18] poly(*N*,*N*-dimethylacrylamide) (PDMA),[16,19] poly(vinylpyrrolidone) (PVP),[16,19] and poly(oxazolines).[19,20]

It has been observed that the interactions between the inorganic oxide and the polymer affect the viscoelastic relaxations of the latter. In composites of PMMA with polymerized tetraethoxysilane (TEOS), the tan δ peak of the α relaxation, observed by dynamic mechanical spectroscopy, decreases in amplitude and broadens.[15] Solid-state ^{31}P NMR of low glass transition temperature polyphosphazene composites prepared with TEOS reveals that, in these optically clear composites, at least some of the polymer chains have reduced mobility relative to the mobility of the bulk.[21] This was interpreted as originating from the polyphosphazene/inorganic oxide network interface, which is immobilized compared to the bulk polymer. In the present study we have chosen to examine the dielectric and viscoelastic response at T_g of acid-catalyzed composites of PVAc and polymerized TEOS. PVAc was chosen since it has shown strong interactions with the silicate network and because its sub-T_g β relaxation peak is far enough removed from the α relaxation to ensure deconvolution of the two motional mechanisms with dielectric spectroscopy. The purpose of the work is to elucidate how the silicate network influences the relaxation mechanisms of PVAc. It will be shown that the local environment of the PVAc chains is affected by the formation of the silicate network. The silicate network acts to increase the distribution of relaxation times of the polymer chains in the glass transition region. This is presumably the result of strong interactions between the two phases and possible interpenetration of the polymer chains in the growing silicate network that effectively restricts the mobility of the PVAc chains.

Experimental Section

The PVAc was purchased from Polysciences, Inc., and was used without further purification. Size-exclusion chromatography shows that the absolute number- and weight-average molecular weights for the PVAc are 63K and 218K, respectively. FTIR analysis showed no evidence of the presence of hydroxyl groups. The tetraethoxysilane was purchased from Petrarch and was also used without further purification.

The composite solutions were prepared by the addition, under continuous mixing, of TEOS to a 20 wt % solution of PVAc in THF, followed by the addition of a stoichiometric amount of water (based on the number of hydrolyzable alkoxide substituents) in the form of 0.15 M HCl. The solutions were mixed at ambient temperature for 65 h prior to coating. Samples for

0024-9297/92/2225-3715$03.00/0

Table I
Composition of PVAc/TEOS Composite Samples

sample	TEOS (wt %)	SiO_2 (wt %) calcd	SiO_2 (wt %) from NA anal.[a,b]
PVAc	0	0.0	0.0
PVAc-5	15.5	5.0	5.1
PVAc-10	27.8	10.0	10.1
PVAc-15	38.0	15.0	14.6
PVAc-20	46.4	20.0	19.9
PVAc-60	83.9	60.0	51.6

[a] NA = neutron activation analysis of the cured composite. [b] The percent SiO_2 was calculated based on the silicon content determined from the NA results.

dielectric studies were obtained by knife coating the solutions onto aluminum-coated Kapton polyimide film. The coatings were dried and cured at 100 °C for 20 h under vacuum or as described in the text. Finally, a second electrode (gold) was evaporated onto the surface of the sample, and the dielectric measurements were performed. The final composite thickness typically varied from 15 to 30 μm. The samples for dynamic mechanical analysis (DMA) were prepared by knife coating the above solutions onto Kapton polyimide film, drying, and curing the composite identically to the dielectric samples and removing the composite films from the substrate. The thickness of these composites was generally between 70 and 100 μm. Samples for infrared analysis were prepared by spin coating the composite solutions onto KBr disks, drying, and curing as described in the text.

The compositions of the composites studied are given in Table I. The samples will be referred to in this work as PVAc-X where X is the nominal weight percentage of SiO_2. These numbers were calculated assuming the total conversion of the TEOS to SiO_2. This is done only as a convenience since it is understood that the inorganic phase is not fully densified. The weight percent of Si was also determined from neutron activation (NA) analysis. These results are presented in Table I along with the concentration of SiO_2 calculated from the initial starting materials.

Measurement of the dielectric loss was made with a Hewlett-Packard Model 4192a impedance analyzer interfaced with an IBM computer. At each temperature, 20 frequencies were measured between 10^2 and 10^6 Hz. The temperature was controlled with an environmental chamber [Delta Design oven (9023)].

The dynamic mechanical properties of the composite were measured using a Rheometrics Solid Analyzer (RSA-II). The driving frequency was 1 Hz, and the temperature was typically scanned between −150 and +300 °C at a rate of 2–3 °C/min.

Fourier transform infrared (FTIR) spectra were obtained using a Bio-Rad (Digilab Division) FTS-7 spectrometer (3240-SPC). The resolution used was 4 cm^{-1}.

The sample for transmission electron mciroscopy (TEM) was sectioned with a diamond knife at 23 °C, giving a section approximately 50 nm thick. TEM was performed using a Philips 400T microscope. The intrinsic contrast between the organic polymer and the SiO_2 network was sufficient, and no staining was required.

Results and Discussion

In a previous study, a composite was formed by the acid-catalyzed hydrolysis and condensation of TEOS in the presence of PMMA. Transmission electron micrographs (TEM) showed that the TEOS polymerized into particles that were <10 nm.[15] In these composites, hydrogen bonding (observed by FTIR) between the carbonyl group of the polymer and the residual silanols on the surface of the silicate network was believed to be very important in controlling the morphology of the composites by retarding phase separation between the organic and inorganic components.[15,16] In the previous references, PMMA was found to be adsorbed to the surface of the silicate phase, as well as entrapped within it. With the use of dielectric spectroscopy it may be possible to elucidate how the silicate network affects the polymer chain relaxations. However, because it is difficult to deconvolute the α and β (sub-T_g) relaxations of PMMA using dielectric spectroscopy,[22] we have chosen to study PVAc as the organic portion of this blend.

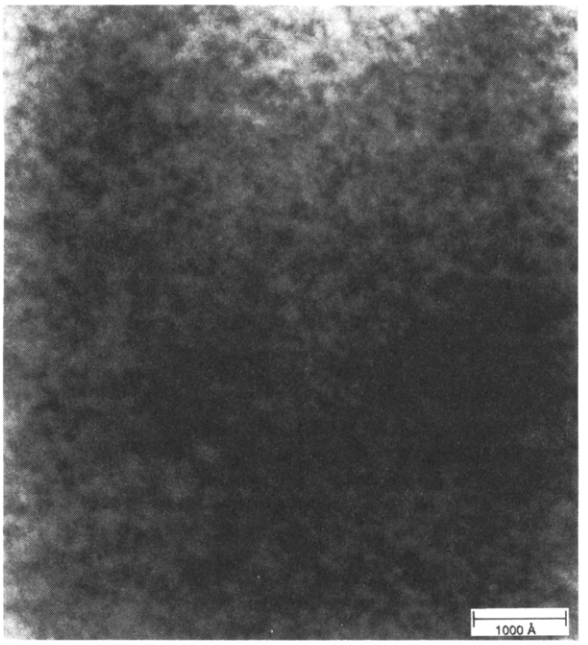

Figure 1. Transmission electron micrograph of the PVAc-15 composite.

The composites formed from the acid-catalyzed polymerization of TEOS in the presence of PVAc are optically clear. Due to the relatively large difference in the refractive index between PVAc and SiO_2, the optical clarity is thought to be due to the small domain size of the SiO_2 particles. This conclusion is similar to previously reported results for PMMA composites.[15] The transmission electron micrograph shown in Figure 1 shows that the SiO_2 exists in a separate phase for the PVAc-15 composite. The dark regions in the micrograph are rich in SiO_2 particles. A qualitative assessment of the micrograph shows that these particles have condensed into both chainlike and spherical structures. Since the particles are extremely small, it is not possible to determine if these domains are single particles or clusters of particles. The micrograph shows that the particles have also condensed into long chainlike structures. These structures appear to be continuous and are seen to be hundreds of nanometers in length, yet only a few nanometers wide. However, since the thickness of the microtoned sample (~50 nm) is much larger than the individual particles, the TEM must be viewed with caution. It is suggested that the observed two-dimensional image may be the result of the random superposition of a three-dimensional structure formed by the stacking of many individual particles. Detailed morphological studies are presently in progress using small-angle X-ray scattering.

The hydrogen-bonding interactions between the silicate phase and PVAc can be seen by FTIR. Figure 2a shows the carbonyl stretching region of PVAc compared with that of two PVAc/TEOS composites (PVAc-20 and PVAc-60). Due to the high silicate content of the PVAc-60 composite, only extremely thin spin coatings could be made without cracks. As seen in the figure, the carbonyl stretch of PVAc has a single well-defined band centered at 1737 cm^{-1}. Both composites show an additional band at 1711 cm^{-1}, which is attributed to a hydrogen-bound carbonyl. The fraction of hydrogen-bound carbonyls for each composite can be determined by fitting the spectra to two bands and correcting the areas for differences in absorptivity. The value for the absorptivity ratio a_{hb}/a_f used for these calculations was 1.5. This value has been reported

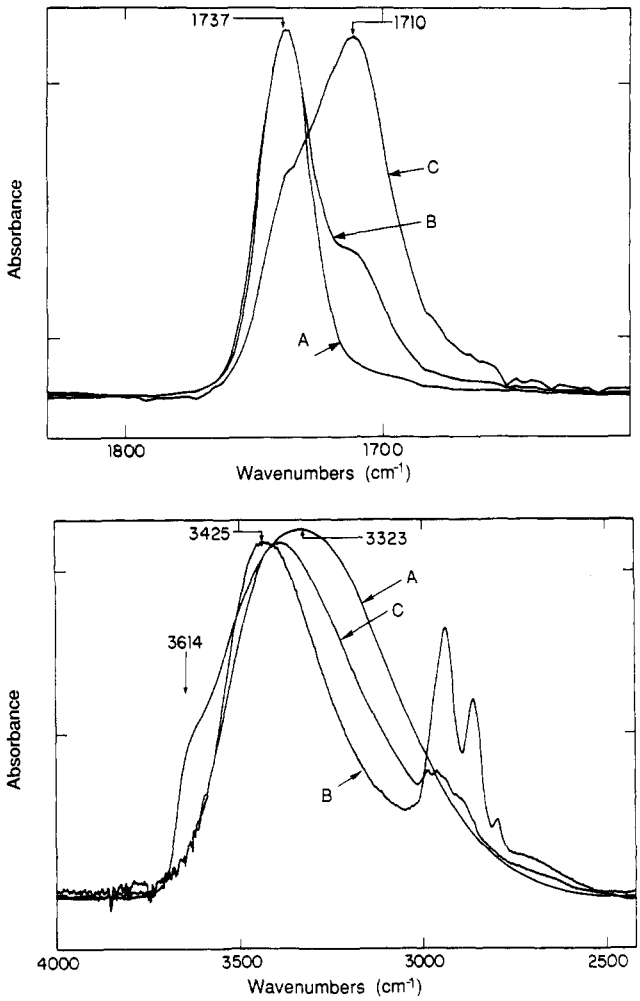

Figure 2. (Top) FTIR of the carbonyl region of (A) PVAc, (B) PVAc-20, and (C) PVAc-60. (Bottom) FTIR of the hydroxy region of (A) TEOS, (B) PVAc-20, and (C) PVAc-60.

for blends of PVAc and poly(vinylphenol) where the carbonyl band of PVAc shows a shift, due to hydrogen bonding, that is of similar magnitude to the one observed for these PVAc/TEOS composites.[23] A similar value for a_{hb}/a_f can be calculated from reported absorptivity coefficient values for free carbonyl and carbonyl that is hydrogen bound to a silica surface for alkyl methacrylate polymers.[24,25] As seen in Table II, whereas only 24% of the carbonyls are hydrogen-bound, initially at 25 °C, in PVAc-20, 76% are associated in the composite with the higher silicate content, PVAc-60.

The participation of the hydroxyl (OH) groups of the silicate in the heteroassociations can be seen by the examination of the OH stretching region. This is shown in Figure 2b where the OH band of pure TEOS, acid-catalyzed and dried at 60 °C, is compared to those of the two composites. The OH band is broad and is composed of overlapping bands for free hydroxyls (ca. 3600 cm^{-1}) and self-associated (dimers and multimers) hydroxyls (ca. 3100–3500 cm^{-1}). For the pure silicate, one observes a significant amount of free hydroxyls contributing to the spectrum that disappears when the PVAc is added. The maximum in the OH band for the composites also shifts to higher frequency as PVAc is added to the silicate, indicating that this heteroassociation is not as strong as the self-association that was present between the silanols. The C=O stretch second overtone peak for PVAc (that occurs at 3455 cm^{-1}) has been substracted from the spectra for the composites.

While FTIR can be used to look at specific interactions between molecules, dielectric and dynamic mechanical spectroscopy can provide complementary information and a greater understanding of the local environment of the relaxing species. The dielectric relaxation behavior of PVAc has been well studied, and it is possible to separate the α from the sub-T_g relaxations in the frequency range of interest.[26-28] The classical Debye equations can often be used to represent the dielectric response of a polymer and are shown in eqs 1 and 2.[22] In these equations, ϵ' is

$$\epsilon'(\omega) = \epsilon_\infty + \frac{\epsilon_0 - \epsilon_\infty}{1 + \omega^2\tau^2} \quad (1)$$

$$\epsilon''(\omega) = (\epsilon_0 - \epsilon_\infty)\frac{\omega\tau}{1 + \omega^2\tau^2} \quad (2)$$

the dielectric constant and ϵ'' is the loss factor, ϵ_0 is the relaxed permittivity (low-frequency dielectric constant), and ϵ_∞ is the unrelaxed permittivity (or the high-frequency dielectric constant). ω is the angular frequency, and τ is the characteristic relaxation time.

The loss factor vs temperature curves, in the vicinity of the α relaxation for pure PVAc and two composites, are shown in Figure 3. The curves are presented to show that the loss curve changes with increasing concentration of SiO_2. The breadth of the loss curve and the temperature at which the maximum in loss occurs are seen to increase with increasing concentration of SiO_2. However, the onset of the relaxation peak appears to be similar for all the materials. The implications of this are discussed later along with the DMA data.

The results show that when ϵ'' is plotted vs log frequency, all the samples exhibit a single absorption peak. However, at high concentrations of SiO_2, there is a steep increase in ϵ'' at low frequencies. An example of these two features is shown in Figure 4. The absorption peak can be attributed to the α relaxation of the dipoles, but the increase in ϵ'' at low frequencies may be a manifestation of either a second peak, suggesting the presence of another phase, or dc conductivity.

In the absence of a dipolar contribution to the loss factor, dc conductivity can give rise to a frequency dependence of ϵ'' that is proportional to $1/\omega$. In this case, the total loss factor is equal to

$$\epsilon''_{total} = \epsilon''_{dipolar} + \epsilon''_{dc} \quad (3)$$

where

$$\epsilon''_{dc} = \sigma/\epsilon\omega \quad (4)$$

σ is the bulk ionic conductivity, ϵ is the permittivity of free space, and ω is equal to $2\pi f$ where f is the frequency. When log ϵ'' is plotted vs log f (not shown), at low frequencies a slope of nearly −1.0 is calculated, suggesting that the upturn is associated with dc conductivity and not a second phase. Therefore, the dc conductivity can be subtracted from the loss factor, and the subtracted curve is shown in Figure 5.

There have been a number of formalisms that have been used to describe the absorption peak associated with the α relaxation process. In these experiments we have chosen to fit our data to the empirical function that was first applied to polymers by Williams and Watts.[29-31] The empirical Kohlrausch–Williams–Watts (KWW) function is intermediate between those of the Cole–Cole and Davidson–Cole functions and has been shown to model the nonsymmetrical loss peak quite well. In these studies all the theoretical curves were generated from the tabulated data of Moynihan et al.[32]

Table II
FTIR Results for the PVAc/TEOS Composites

sample (% SiO_2)	T (°C)	ν(C=O) f	ν(C=O) hb	area f	area hb	% C=O hb[a]	% C=O hb[b]
20	25	1737.1	1710.3	6.33	2.93	31.6	23.6
	50	1737.6	1711.3	6.10	3.11	33.8	25.4
	100	1738.5	1712.9	6.37	2.30	26.5	19.4
	150	1739.5	1714.8	6.49	1.68	20.5	14.7
	200	1740.4	1715.3	6.58	1.49	18.5	13.1
	25 (ret)	1737.7	1710.9	7.24	1.62	18.2	12.9
60	25	1737.0	1711.0	0.58	2.76	82.3	75.6
	50	1737.2	1711.3	0.57	2.73	82.7	76.1
	100	1737.5	1712.6	0.47	2.71	85.2	79.4
	150	1738.2	1713.9	0.53	2.55	82.8	76.2
	200	1739.8	1715.7	0.89	2.03	69.4	60.2
	250	1741.3	1718.1	0.95	1.36	58.9	48.9
	25 (ret)	1741.5	1714.9	0.95	1.44	60.3	50.5

[a] Determined from the ratio of the areas. [b] Determined using a value of $a_{hb}/a_f = 1.5$.[23]

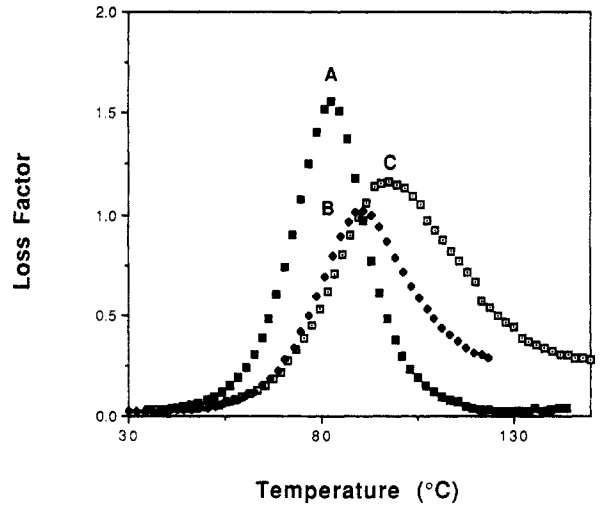

Figure 3. Loss factor vs temperature for (A) PVAc, (B) PVAc-10, and (C) PVAc-15 at 12.742 kHz.

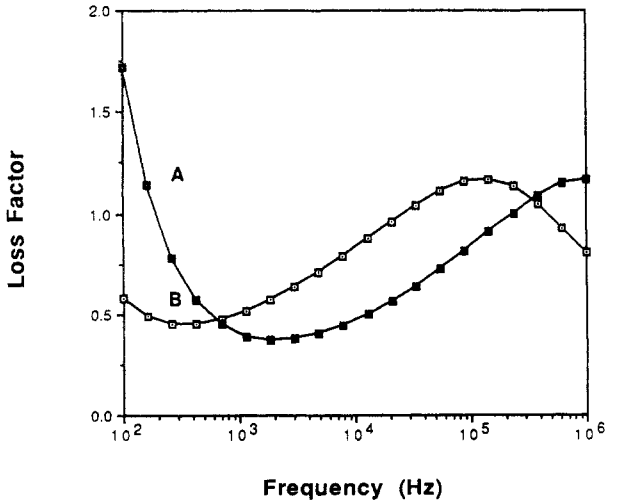

Figure 4. Dielectric loss vs frequency for a PVAc-20 composite at (A) 126 and (B) 112 °C.

The permittivity is then given by

$$\frac{\epsilon^* - \epsilon_\infty}{\epsilon_0 - \epsilon_\infty} = \int_0^\infty \left[\frac{-d\phi(t)}{dt}\right] \exp(i\omega t)\, dt \qquad (5)$$

where $\phi(t)$, the Kohlrausch function,[22] is given by

$$\phi(t) = \exp[-(t/\tau)^\beta] \qquad (6)$$

where β has values of $0 < \beta < 1$. When the distribution parameter β is equal to 1, a single relaxation process is observed. As stated previously, this function was used as an empirical fit, and only recently with the use of a coupling model workers such as Ngai et al.[33,34] have attempted to assign physical meaning to β.

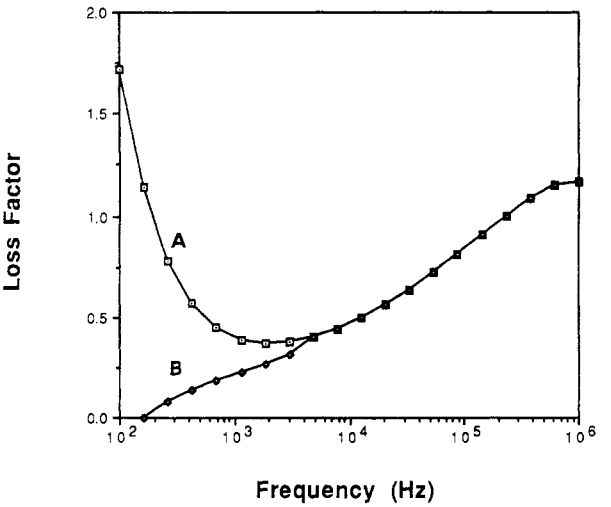

Figure 5. Dielectric loss vs frequency for a PVAc-20 composite at 126 °C (A) before and (B) after the contribution from dc conductivity is removed.

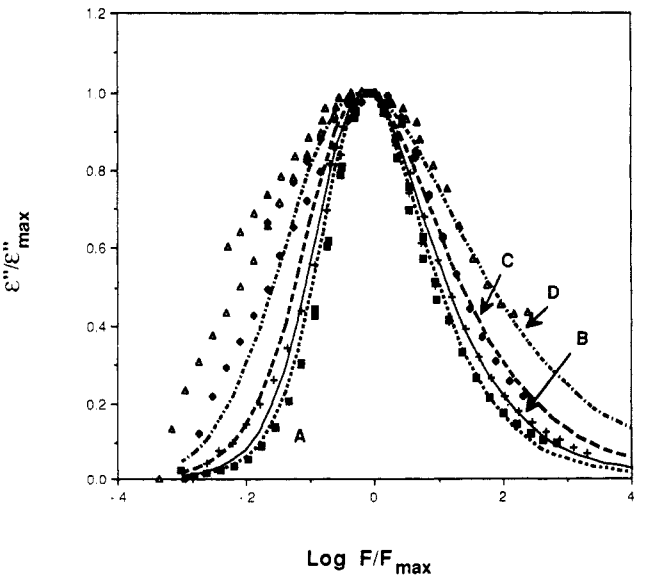

Figure 6. Normalized loss curves for (A) PVAc, (B) PVAc-10, (C) PVAc-15, and (D) PVAc-20. For clarity, the normalized loss curve for PVAc-5 is not shown. The lines represent the best fits for β to the data.

The normalized relaxation or master curves for each of the composites are shown in Figure 6. These curves are much broader than those for a single relaxation time,

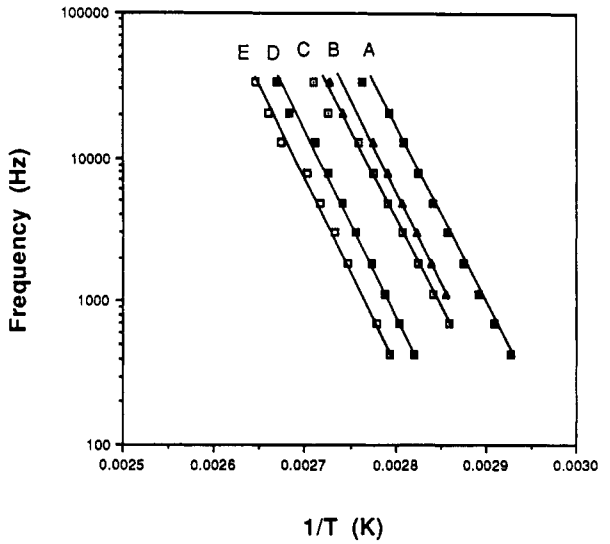

Figure 7. Arrhenius activation plots for (A) PVAc, (B) PVAc-5, (C) PVAc-10, (D) PVAc-15, and (E) PVAc-20.

Table III
Apparent Activation Energy and β as a Function of SiO_2 Content

concn of SiO_2	β	E_{app} (kcal/mol)	concn of SiO_2	β	E_{app} (kcal/mol)
0	0.56	55.4	15	0.42	57.5
5	0.55	53.9	20	0.32	60.0
10	0.50	55.0			

indicating that the polymer chains exhibit a distribution of relaxation times. This behavior is typical of amorphous polymers since the dipole mobility along the polymer chain is a function of the molecular weight, the proximity to the chain ends, and the surrounding environment. Analysis of the normalized loss factor data for PVAc using the KWW function indicates that a β of 0.56 fits the experimental data well. This value is similar to the value of β reported previously by Williams et al. for PVAc.[30]

The results show that as the concentration of SiO_2 increases the normalized loss curves broaden and, as shown in Table III, the best fit value for β decreases. Since β can be qualitatively considered a measure of the distribution of environments of the dipoles, the results suggest that the local environment of the dipoles along the PVAc chain is influenced by the presence of the silicate network. At concentrations less than and equal to 10 wt % SiO_2, it is possible to shift the data along the frequency axis. However, for the samples containing 15 and 20 wt % SiO_2 the results show that it is possible to fit the high-frequency side of these loss curves reasonably well. However, the low-frequency side of the loss curves exhibits extensive broadening even after removing the contributions from dc conductivity, and it is not possible to superpose the data obtained at different temperatures. We believe low-frequency broadening of these curves and breakdown of the time–temperature superposition principle are manifestations of polymer chains that are trapped within the silicate network. These interactions can be responsible for restricting the motion of the PVAc polymer chains in their surrounding environment, thus creating a lower frequency relaxation. This lower frequency relaxation would manifest itself in isochronal experiments as a broadening to the high-temperature side of the relaxation. Thus the local environment of the PVAc in these composites is microheterogeneous, in that the interacting polymer chains pose a slower relaxation time as compared to those chains in a more mobile environment.

While the data in Figure 7 show a slight downward curvature, the temperature–frequency regime studied is not large enough to assign this to WLF behavior for the glass transition. Apparent activation energies (E_{app}) were therefore calculated for all the blends studied. As shown in Figure 7, frequency is plotted vs $1/T$, where T is the temperature corresponding to the maximum of ϵ'' at that frequency. Calculations indicate that the activation energy for PVAc is 55.4 kcal/mol and is in agreement with Mashimo et al.,[26] who calculated an activation energy of 59 kcal/mol. As seen in Table III, the apparent activation energy for the glass transition of the blends varies between 54 and 60 kcal/mol and is similar to the activation energy of the pure PVAc. In fact, the results indicate that only the preexpoential factor of the E_{app} changes with increasing concentration of SiO_2.

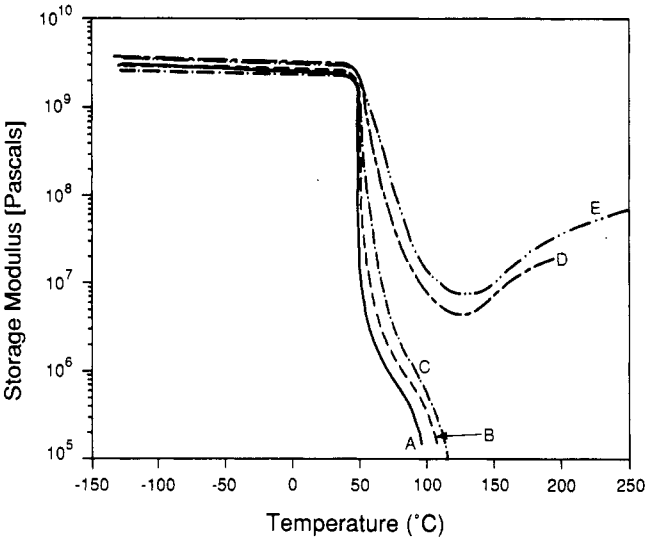

Figure 8. Storage modulus vs temperature for (A) PVAc, (B) PVAc-5, (C) PVAc-10, (D) PVAc-16, and (E) PVAc-20. For clarity smooth lines have been drawn through the data.

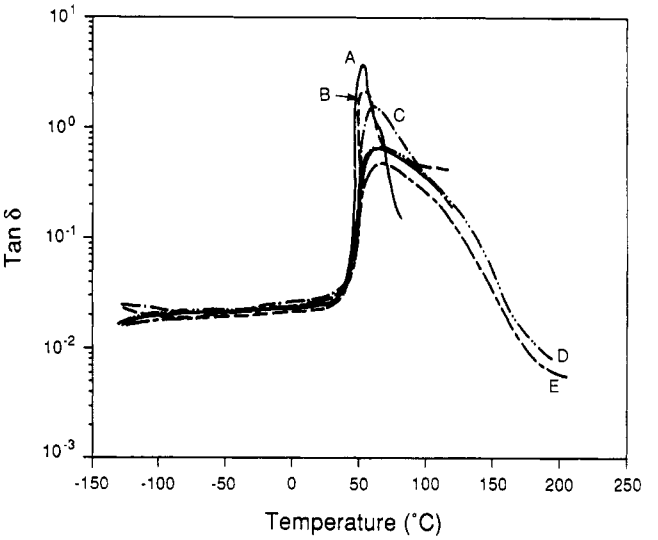

Figure 9. Tan δ vs temperature for (A) PVAc, (B) PVAc-5, (C) PVAc-10, (D) PVAc-15, and (E) PVAc-20. For clarity smooth lines have been drawn through the data.

The results of the dynamic mechanical analysis studies are shown in Figures 8 and 9. From the storage modulus vs temperature plots, it can be seen that PVAc and the composites containing less than 10 wt % SiO_2 undergo viscous flow above T_g. However, composites formed containing 15 and 20 wt % SiO_2 exhibit a plateau modulus above T_g that is greater than 10^7 Pa and persists up to temperatures as high as 300 °C. The formation of a plateau is consistent with the formation of a continuous silicate network structure. It should be noted that at the concentrations of SiO_2 that a plateau modulus is observed

time–temperature superposition of the dielectric data does not occur.

In addition, from the tan δ vs temperature plots, Figure 9, it can be seen that there is no change in the onset of the glass transition temperature (as reflected by the α peak) relative to that of the pure PVAc. However, considerable broadening is seen to occur on the high-temperature side of the α relaxation. Thus, although the distribution of relaxation times for the PVAc motion is broadened, the fast edge of the distribution remains situated at approximately the same place in the composites as in the pure polymer.

The dielectric and DMA results indicate that portions of the PVAc polymer chains are affected by the addition of the SiO_2 component whereas many chains remain unaffected by its presence. The results suggest that an environment exists wherein the PVAc chains interact strongly with the silicate network, thus increasing the barriers to the relaxational mode at T_g and shifting the relaxation to higher temperature. Whether the restricted environment is due to specific interactions (hydrogen bonding) or interpenetration of the polymer with the tightly cross-linked silicate network has not been definitively determined.

There is some indication from the DMA studies that TEOS continually reacts at an elevated temperature during the DMA experiment. The increase in the storage modulus, shown in Figure 8, in the plateau region occurs too rapidly to be consistent with the molecular theory of rubber elasticity.[35] Presumably because the initial curing is done at 100 °C, condensation of the TEOS is not complete. Therefore, as the temperature is raised above the curing temperature of the composite, the sol–gel can continue to react. Cross-reactions between the PVAc and the SiO_2 at higher temperatures are a possibility and must be considered.

Head-space analysis was performed by incubating the samples at temperatures of 100, 150, 200, or 250 °C for 2 h in air and then analyzing the volatiles by GC–MS. In particular, the presence of acetic acid was of interest. This would be the product formed by the silicate-surface-catalyzed cleavage of the C–O (ether) bond and the formation of covalent bonds between the silicate and the organic polymer backbone. At 100 °C no acetic acid was detected. At 150 °C, less than 0.2 mol % of the acetate groups evolved. However, at 200 °C, up to 4 mol % of the acetate groups evolved, and at 250 °C the samples turned yellow and a substantial amount of acetic acid was detected. Moreover, while at temperatures below 150 °C only a little acetic acid is detected, there is a possibility that hydrolysis of the PVAc had occurred. This may result in the formation of Si–OAc bonds or acetic acid that would be difficult to remove from the network because of its ability to hydrogen bond with the network. Further analysis of the total area of the carbonyl peak (free plus hydrogen-bound (corrected for a_{hb}/a_f)) at 25 °C (by FTIR) for PVAc/TEOS samples before and after heating to 200 °C indicates that there is no detectable change in the total number of carbonyls in the composite.

Curing Studies. It is expected that the temperature at which the composites are cured would affect the molecular and dipolar relaxations of the composite. Therefore, samples of PVAc-15 were prepared as described above and cured at 52, 100, 150, and 200 °C. The dielectric master curves, Figure 10, show that the temperature at which the samples are cured affects the breadth of the relaxation curve. The value of β is seen to increase with increasing cure temperature. This would indicate that the local environment of the polymer chains becomes more homogeneous as the cure temperature is increased. Possibly

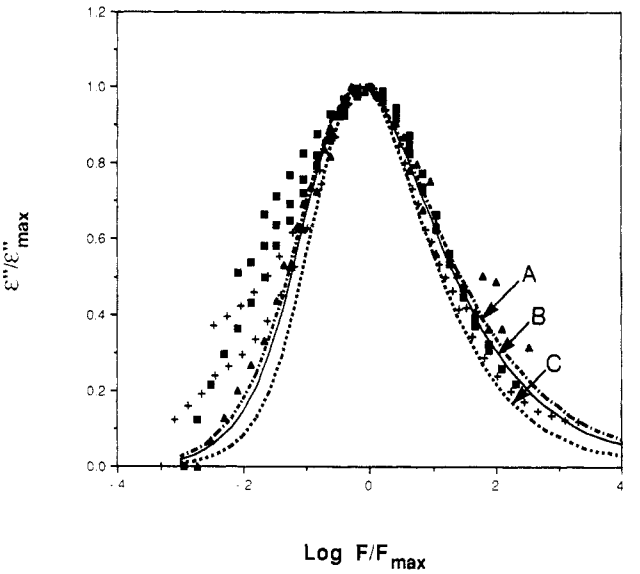

Figure 10. Normalized master curves after the contribution to dc conductivity is removed for PVAc-15 cured at (A) 52, (B) 100, and (C) 150 °C.

Table IV
Effect of Cure Temperature for PVAc-15 on E_{app} and β

cure temp (°C)	β	activation energy (kcal/mol)
52	0.40	50.5
100	0.42	57.5
150	0.50	54.0

this is the result of a higher extent of reaction of the condensing silicate network that may limit the number of environments available to the PVAc chains. Some chains may find their mobility reduced to the extent that their relaxation no longer occurs in the experiment at an observable frequency or temperature range and, therefore, do not participate in the primary α transition being examined here. As discussed earlier, it is possible to fit the high-frequency side of the master curve, but the low-frequency side exhibits extensive broadening.

The E_{app} for this process was calculated as described earlier and is shown in Table IV. The results indicate that the cure temperature only influences the preexponential of the activation energy for the glass transition and the activation energy is seen to vary between 50.5 and 57.5 kcal/mol. These activation energies are within our experimental error and sample-to-sample reproducibility.

The DMA curves (shown in Figures 11 and 12) for the PVAc-15 cure series support the dielectric results. The tan δ loss peaks narrow as the cure temperature is increased. The magnitude of E' in the rubbery plateau is also shown to increase with cure temperature, but all the samples come to a common value of E' at about 230 °C. For the composites that were cured at the higher temperatures, the rise in E' with temperature is not as steep as observed for the 100 °C cured samples.

Although condensation of the silicate network does proceed during thermal treatment at these low temperatures (100–150 °C) as shown by ^{29}Si NMR of a similar system (PMMA/TEOS composites),[16] it is known that densification of the glass does not occur to any significant extent (at least for base-catalyzed TMOS[36]) until a much higher temperature is reached. Therefore, the rapid upturn in E' between ~80 and 150 °C (for the sample cured at 100 °C (Figure 11, sample A)) could be attributed to a combination of network condensation and solvent loss (THF, ethanol, and water). Head-space chromatography does reveal the presence of ~6 wt % residual THF

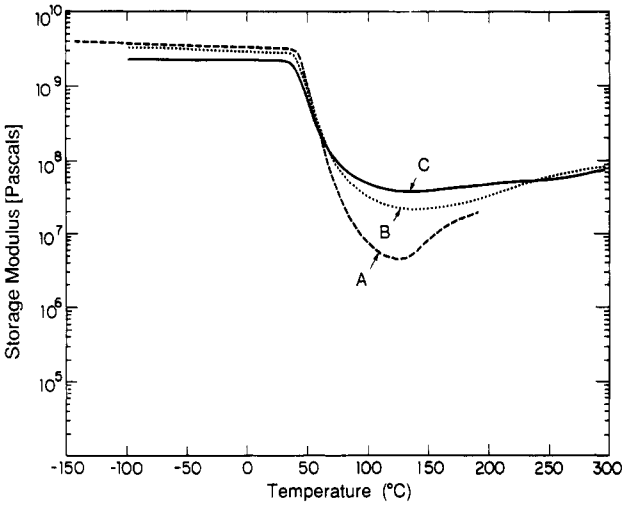

Figure 11. Storage modulus vs temperature plots for the sample of PVAc-15 cured at (A) 100, (B) 150, and (C) 200 °C for 20 h. For clarity smooth lines have been drawn through the data.

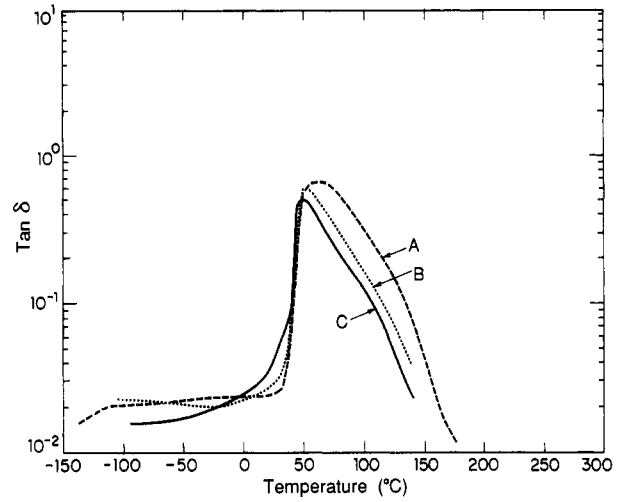

Figure 12. Tan δ vs temperature plots for the sample of PVAc-15 cured at (A) 100, (B) 150, and (C) 200 °C for 20 h. For clarity smooth lines have been drawn through the data.

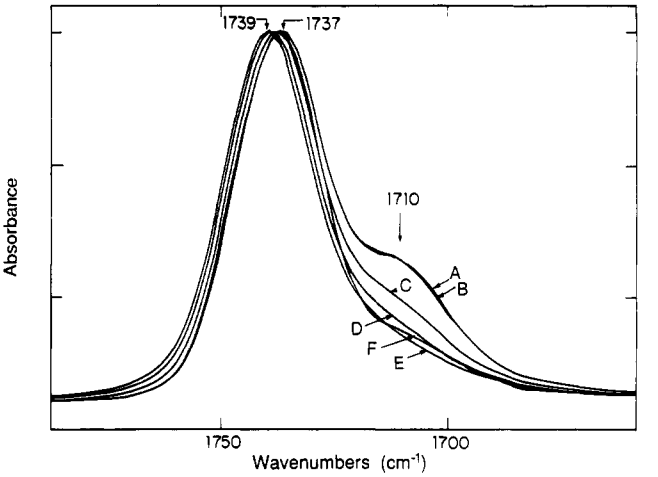

Figure 13. FTIR spectra of the carbonyl regions of the PVAc-20 composite acquired at increasing temperatures (A) 25, (B) 50, (C) 100, (D) 150, and (E) 200 °C and (F) then cooled back to 25 °C.

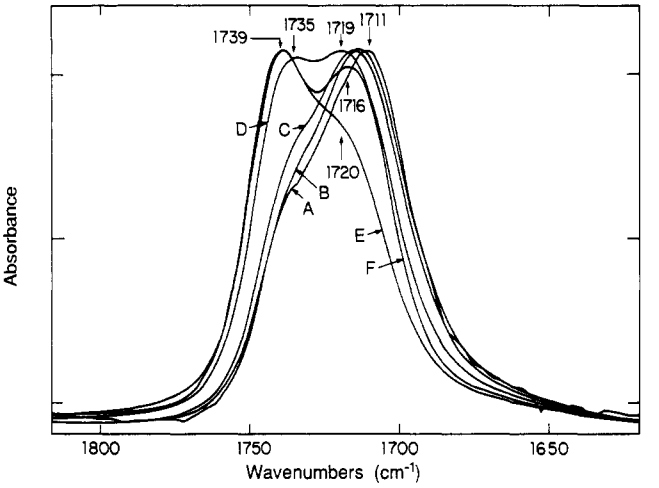

Figure 14. FTIR spectra of the carbonyl regions of the PVAc-60 composite acquired at increasing temperatures (A) 25, (B) 50, (C) 100, (D) 150, and (E) 200 °C and (F) then cooled back to 25 °C.

that comes out at ca. 150 °C for this sample even though it had been cured at 100 °C for 20 h under vacuum.

This residual solvent is most probably associating with the silicate network and not with the PVAc chains since no depression in the T_g of PVAc is observed. Also if one looks carefully at Figure 2b and compares the maxima of the absorbance peaks for the silanols in samples of PVAc 20 and PVAc-60, the question arises as to why these two peaks do not coincide. One might speculate that PVAc-60 would retain more THF than PVAc-20 (more network surface area), and if the silanols are hydrogen bonding to both the ester of the PVAc and to the residual THF (ether), the peak (which reflects a combination of both interactions) would occur at lower wavenumbers than if the only interaction was between the silanols and the ester group. This is supported by the fact that the peak maximum for PVAc-60 does undergo a slight irreversible shift to higher wavenumbers after the sample is cured to 250 °C.

FTIR was used to monitor the changes in hydrogen bonding that occur during the curing of the PVAc-20 and PVAc-60 composites. The spectra were acquired at increasing temperatures between 25 and 200 or 250 °C. The samples were then cooled back to 25 °C and their spectra taken once again. The results are shown in Figures 13 (PVAc-20, carbonyl region) and 14 (PVAc-60, carbonyl region) and in Table II. As the temperature is raised, the amount of hydrogen bonding (both heteroassociation and self-association) decreases. This is consistent with the fact that the hydroxyls are condensing with each other, thus reducing the total number of OH groups available to participate in hydrogen bonding. When the sample is brought back to 25 °C, the amount of hydrogen bonding increases due to the decrease in thermal energy which increases the strength of the intermolecular interactions but is not totally reversible. The fraction of carbonyls that are hydrogen bound can be calculated by fitting the spectra to two bands and correcting for differences in the absorptivities of the free and bound carbonyl vibrations. An irreversible shift to higher frequency (of about 4 cm^{-1}) in the peak positions of both the free and bound carbonyl stretching vibrations is observed after heating the PVAc-60 composite to 250 °C. This is probably due to some chemistry occurring between the PVAc and the silicate that results in confining the motions of the PVAc carbonyls. The position of the carbonyl peak for the PVAc-20 composite, which was heated to 200 °C only, was however, found to be reversible.

Conclusions

The local environment of PVAc chains in the sol–gel composites prepared with TEOS has been probed using FTIR, dielectric, and dynamic mechanical spectroscopy. The results suggest that the PVAc and silicate networks interact strongly, thus restricting the molecular motions

of the PVAc chains. The DMA and dielectric data suggest that the onset of the glass transition temperature does not vary with increasing concentration of TEOS. However, there is considerable broadening of both the dielectric and dynamic mechanical absorption peaks. From the dielectric data, master curves were constructed and the empirical KWW function was fit to the data. The distribution parameter β was seen to decrease with increasing concentration of TEOS, indicating a broader distribution of relaxation times.

The activation energy for the glass transition process was essentially the same for all the composites studied. In addition, the activation energy is similar to that of pure PVAc. The dielectric and dynamic mechanical studies taken together suggest that the in-situ polymerized silicate network inhibits the relaxation of at least a portion of the PVAc chains. This results in a broadening in the distribution of relaxation times for PVAc chains. However, both DMA and dielectric studies indicate that the fast edge of this distribution remains unchanged. One must consider, however, that this change in the distribution is in part only a statistical phenomenon. At these low SiO_2 concentrations, a certain portion of PVAc chains in the composite will remain largely surrounded by PVAc chains and the motions of these chains will be unaffected.

The dielectric and DMA results also show that as the composite is cured at higher temperatures the distribution of relaxation times narrows. This suggests that there exists an interfacial region in these composites where the mobility of the PVAc chains is reduced by the interactions with the silicate network. However, as the silicate network condenses, these PVAc chains are restricted to a greater extent so that their relaxations are no longer observable on the time scale of these dynamic experiments, leaving the relaxations of the unperturbed chains to dominate the spectra. As the composite is cured, it is also shown that the amount of hydrogen bonding between the PVAc and the silicate networks decreases. This is due to further condensation of the silicate and the proportional decrease in available OH sites. However, the high modulus rubber plateau in E' persists to temperatures where there is very little hydrogen bonding remaining, suggesting that there is an additional reinforcement mechanism at work, possibly entrapment of the PVAc chains within the silicate network. Thus, hydrogen bonding between the organic polymer and the silicate network is believed to be important in preventing phase separation and controlling the morphology prior to vitrification. It may also contribute somewhat to the reinforcement of the polymer; however, entrapment of the chains by the silicate network and the nature of the network itself are ultimately thought to be the essential mechanism for reinforcement.

There does not seem to be any evidence for substantial cross-reactions between the PVAc and the silicate network at temperatures as high as 150 °C. Head-space analysis of the volatiles and FTIR measurements at those temperatures indicate the possibility of a few percent reaction occurring that would be difficult to detect. At higher temperatures, cross-reactions are highly possible. These could contribute to the plateau modulus and further reinforcement of the composite.

Acknowledgment. We thank Dr. Wilson Yetter for the TEM and Mr. Joseph Sedita and Dr. James O'Reilly for conversations concerning the KWW function. We also express our appreciation to Ms. Robynn Schillace for making the dielectric measurements and Dr. Bradley Coltrain for valuable discussions.

References and Notes

(1) Schmidt, H.; Kaizer, A.; Patzelt, H.; Scholze, H. *J. Phys. Colloq.* **1982**, *C9*, 275 (also U.S. Patents 4,322,517 (1982) and 4,440,745 (1984)).
(2) Schmidt, H. *J. Non-Cryst. Solids* **1985**, *73*, 681.
(3) (a) Coltrain, B. K.; O'Reilly, J. M.; Turner, S. R.; Sedita, J. S.; Smith, V. K.; Rakes, G. A.; Landry, M. R. *Proceedings of the 5th Annual International Conference on Crosslinked Polymers*; Switzerland, 1991; p 11. (b) Coltrain, B. K.; Rakes, G. A.; Smith, V. K. U.S. Patent 5,019,607, 1991.
(4) (a) Huang, H. H.; Orler, B.; Wilkes, G. L. *Macromolecules* **1987**, *20*, 1322. (b) Huang, H. H.; Orler, B.; Wilkes, G. L. *Polym. Bull.* **1985**, *14*, 557.
(5) Huang, H. H.; Glaser, R. H.; Wilkes, G. L. *ACS Symp. Ser.* **1988**, *360*, 354.
(6) Brennan, A. B.; Wilkes, G. L. *Polymer* **1991**, *32*, 733.
(7) Wang, B.; Wilkes, G. L.; Hedrick, J. C.; Liptak, S. C.; McGrath, J. E. *Macromolecules* **1991**, *24*, 3449.
(8) Sun, C.-C.; Mark, J. E. *Polymer* **1989**, *30*, 104.
(9) Mark, J. E. *Br. Polym. J.* **1985**, *17*, 144.
(10) Jiang, C.-Y.; Mark, J. E. *Makromol. Chem.* **1984**, *185*, 2609.
(11) Clarkson, S. J.; Mark, J. E. *Polym. Commun.* **1987**, *28*, 249.
(12) (a) Mauritz, K. A.; Jones, C. K.; Warren, R. M. *Polym. Mater. Sci. Eng.* **1988**, *58*, 1079. (b) Mauritz, K. A.; Jones, C. K. *J. Appl. Polym. Sci.* **1990**, *40*, 1401.
(13) Mauritz, K. A.; Storey, R. F.; Jones, C. K. In *Multiphase Polymers: Blends and Ionomers*; *ACS Symposium Series* 395; Utracki, L. A., Weiss, R. A., Eds.; American Chemical Society: Washington, DC, 1989.
(14) (a) Coltrain, B. K.; Ferrar, W. T.; Landry, C. J. T. U.S. Patent 5,010,128, 1991. (b) Coltrain, B. K.; Ferrar, W. T.; Landry, C. J. T.; Molaire, T. R. *Polym. Prepr. (Am. Chem. Soc., Div. Polym. Chem.)* **1991**, *32* (2), 477. (c) Landry, C. J. T.; Coltrain, B. K. U.S. Patent 5,051,298, 1991.
(15) (a) Landry, C. J. T.; Coltrain, B. K.; Brady, B. K. *Polymer* **1992**, *33*, 1486. (b) Landry, C. J. T.; Coltrain, B. K. *Polym. Prepr. (Am. Chem. Soc., Div. Polym. Chem.)* **1991**, *32* (2), 514.
(16) Landry, C. J. T.; Coltrain, B. K.; Wesson, J. A.; Zumbulyadis, N.; Lippert, J. L. *Polymer* **1992**, *33*, 1496.
(17) Bechtold, M. F. U.S. Patent 2,404,357, 1946.
(18) LeBoeuf, A. R. U.S. Patent 3,971,872, 1976.
(19) Saegusa, T.; Chujo, Y. Proceedings for the 33rd IUPAC Meeting on Macromolecules, Montreal, 1990.
(20) (a) David, I. A.; Scherer, G. W. Proceedings for the 33rd IUPAC Meeting on Macromolecules, Montreal, 1990. (b) David, I. A.; Scherer, G. W. *Polym. Prepr. (Am. Chem. Soc., Div. Polym. Chem.)* **1991**, *32* (2), 514.
(21) Coltrain, B. K.; Ferrar, W. T.; Landry, C. J. T.; Molaire, T. R.; Zumbuyladis, N. *Chem. Mater.* **1992**, *4*, 358.
(22) McCrum, N. G.; Read, B. E.; Williams, G. *Anelastic and Dielectric Effects in Polymeric Solids*, John Wiley: New York, 1967.
(23) Moskala, E. J.; Howe, S. E.; Painter, P. C.; Coleman, M. M. *Macromolecules* **1984**, *17*, 1671.
(24) Hampton, R. R.; Newell, J. E. *Anal. Chem.* **1949**, *21* (8), 914.
(25) Fontana, B. J.; Thomas, J. R. *J. Phys. Chem.* **1961**, *25*, 480.
(26) Shioya, Y.; Mashimo, S. *J. Chem. Phys.* **1987**, *87*, 3173.
(27) Mashimo, S.; Nozaki, R.; Yagihara, R.; Takeishi, S. *J. Chem. Phys.* **1982**, *77*, 6259.
(28) Rendell, R. W.; Ngai, K. L.; Mashimo, S. *J. Chem. Phys.* **1987**, *87*, 2359.
(29) Williams, G.; Watts, D. C. *Trans. Faraday Soc.* **1970**, *66*, 2503.
(30) Williams, G.; Watts, D. C.; Dev, S. B.; North, A. M. *Trans. Faraday Soc.* **1971**, *67*, 1323.
(31) Kohlrausch, R. *Ann. Phys.* **1847**, *12* (3), 3931.
(32) Moynihan, C. T.; Boesch, L. P.; Laberge, N. L. *Phys. Chem. Glasses* **1973**, *14* (6), 122.
(33) Ngai, K. L.; Rajagopal, A. K.; Teitler, S. *J. Chem. Phys.* **1988**, *88*, 5086.
(34) Ngai, K. L.; Rajagopal, A. K.; Rendell, R. W. *IEEE Trans. Elec. Insul.* **1986**, *E121*, 313.
(35) Ferry, J. D. *Viscoelastic Properties of Polymers*; John Wiley: New York, 1980.
(36) Adachi, T.; Sakka, S. *J. Mater. Sci.* **1990**, *25*, 4732.

Registry No. PVAc, 9003-20-7; $(EtO)_3SiOEt$, 78-10-4; SiO_2, 7631-86-9.